266 nm Laser-Induced Fluorescence Reference Spectra of Ketones and Aromatic compounds

J. Brunzendorf, J. Höltkemeier-Horstmann, D. Markus
Physikalisch-Technische Bundesanstalt (PTB)
Braunschweig, Germany

1 Introduction

Temperature distributions and local gas concentrations are key parameters in combustion processes. Laser-induced fluorescence (LIF) is an established non-invasive measurement method to determine these measurands with high spatial and temporal resolution. For the quantitative interpretation of a LIF spectrum, the influence of temperature, pressure and quencher concentration must be known. This applies in particular to the evaluation of signal ratios such as in two-color thermometry or other multispectral techniques. The dependencies of the fluorescence spectrum must be determined experimentally. A compilation of literature data can be found in the tracer LIF database www.tracer-sim.com [1]. The published LIF spectra differ considerably, even in the case of standard LIF tracers such as acetone at normal conditions (Fig. 1): Here, the position of the LIF intensity maximum of acetone at an excitation wavelength of 266 nm is located at either at 385 nm [2], near 400…410 nm [3-5] with a possible secondary maximum near 370 nm [5] or at 450 nm [6]. The peak normalized fluorescence values for a given wavelength differ by up to a factor of two.

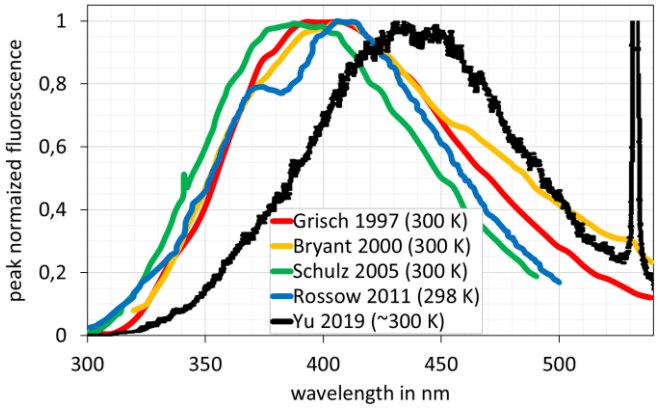

Figure 1: *Literature data of 266 nm LIF spectra of acetone at ambient conditions [1-6]*

Correspondence to: Jens.Brunzendorf@PTB.de

The situation is similar or worse for the other LIF tracers as well as for non-standard conditions. The causes of these discrepancies are believed to be the challenges in measuring and calibrating the LIF spectra, such as low dynamic range and nonlinearities of the image intensifier, inhomogeneous sensitivity distribution across the image intensifier plane (a typical cause is the temporally increasing deterioration due to the incidence of light, for example at the position of strong emission lines of the calibration lamp), significant vignetting of the coupling optics in image intensified cameras, too small detectors that require piecing together the total spectrum from partial spectra ("stitching" or "gluing"), wavelength-dependent absorption of antireflection coated lenses, and calibration issues. Last but not least, stray light is a typical disturbance, especially when using a halogen calibration lamp, which emits primarily in the red and infrared and can cause a lot of stray light accordingly.

In the present work, ambient-condition 266 nm laser-induced fluorescence spectra of three common LIF tracers (acetone, 3-pentanone, toluene) as well as anisole are presented with unprecedented signal-to-noise ratio. By using a large UV-sensitive sCMOS camera instead of an image intensified camera, many of the influencing factors mentioned above could be eliminated. The remaining sources of interference mentioned were carefully considered. Particular care was taken to calibrate the spectra with metrological traceability to the International System of Units SI.

2 Experimental Setup

The spectrometer setup is based on a conventional Czerny-Turner with 320 mm focal length (Acton Research SpectraPro-300i), a grating with 150 lines/mm and a blaze wavelength of 300 nm. An extra aperture is inserted between the last mirror and the detector for additional stray light removal. The spectra were recorded by a scientific CMOS camera containing a Gpixel GSENSE 400BSI sensor with 22×22 mm² area and 11 µm pixel size (2048×2048 pixels, backside-illuminated). Thus, a spectral range from 200 nm to 670 nm is simultaneously covered with a pixel resolution of 0.24 nm/pixel and a measured spectral FWHM resolution of better than 1 nm. With this type of sensor, nonlinearities are not an issue, and readout noise is less than 2 e^-/pixel (sensor temperature -25 °C). The UV quantum efficiency exceeds 30 % above 200 nm.

For the LIF excitation the 266 nm laser light is produced by an Innolas Spitlight 2500 (up to 200 mJ per pulse with 7 ns pulse length and a repetition rate of 3 Hz). The laser beam passes a cylindrical quartz glass gas cell of type Hellma 120-QS (Fig. 2). An 8 mm entrance pupil removes incoming stray light and defines the laser beam cross-section.

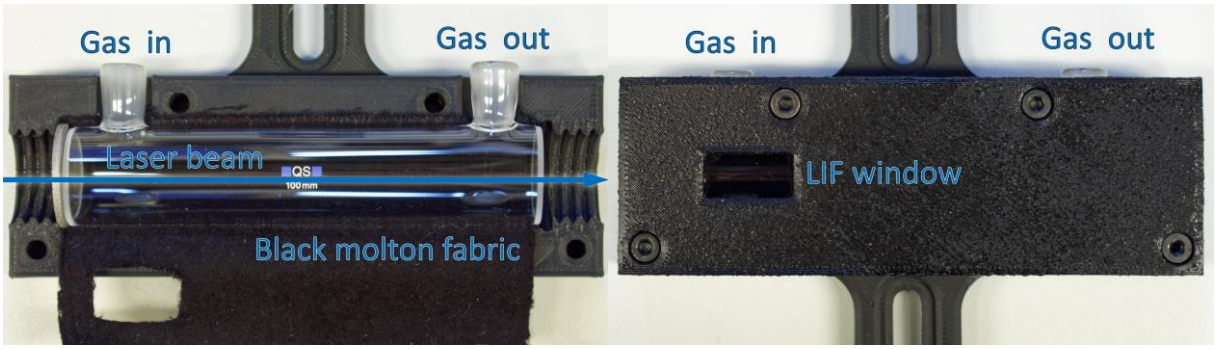

Figure 2: *Quartz cuvette for LIF detection (**Left:** open housing, **Right:** final configuration). Laser beam and gas flow directions: left→right. Black molton wraps cuvette, LIF window below gas entrance.*

This cell is purged with the carrier/tracer gas mixture, which is produced in a temperature-stabilized Drechsel gas wash bottle with filter disk containing the liquid tracer. This bubbler is purged with either nitrogen, hydrogen or dry air at a flow rate of 1 liter/min, corresponding to a gas velocity within the gas cell of 6 cm/s. Hydrogen and nitrogen are supplied via compressed gas cylinders, while the dry air is produced from filtered and dried compressed air. Since the LIF spectra of anisole or toluene in air differ

significantly from their LIF spectra in the oxygen-free carrier gases, these air measurements were repeated using the purest air available (hydrocarbon-free synthetic air from Linde gas cylinders containing 20% O_2, 80% N_2, and less than 0.1 ppm hydrocarbons). This ensures that all differences in the LIF spectra of anisole and toluene are indeed due to the specified carrier gases.

The gas cell is completely wrapped in black molton fabric to absorb stray light with the exception of the laser entrance and exit windows and a side window 2×1 cm² just below the gas entrance. The location of this LIF window next to the gas entrance, the 6 cm/s gas speed and 2 cm window length ensure that fresh tracer gas is measured at each laser shot. The whole lab is kept at a temperature of 1.5 K above the bubbler water bath temperature of 20°C to avoid tracer condensation.

The spectrometer slit entrance is placed next to the gas cell side window, the distance between the laser beam axis and the slit entrance amount to 5 cm. There is no optical element between gas cuvette and spectrometer. Hence, all influences of the light collection optics and anti-reflection coating are eliminated. Note that the emission spectrum of a calibration lamp is different at different points of the lamp and optical elements can either focus on the hottest part of the tungsten wire or the cooler housing, thus changing the measured spectrum.

Great care was taken to avoid LIF-active substances in the setup and to remove all reflections, including within the spectrometer. The surfaces of the setup are painted with black non-fluorescent paint or covered with black molton fabric. An additional housing shields the experiment from ambient light.

3 Measurements and Data Reduction

The calibration of the wavelength axis is based on the emission lines of a mercury vapor lamp of type Newport Spectral Calibration Lamp, Hg (Ar), Model 6035. The positions of the emission lines were taken from the metrological NIST atomic database. The sCMOS sensor is oriented so that the emission lines are parallel to the *x*-axis, while the wavelength axis follows the *y*-axis. A linear fit between the emission line wavelengths and the corresponding y positions of the lines provides the wavelength calibration with an uncertainty of less than 0.2 nm.

For the determination of the spectral response of the setup (intensity calibration), the gas cell is removed and a PTB calibration lamp is placed at a distance of 50 cm from the entrance slit of the spectrometer. All non-black parts outside the light path between lamp and entrance slit were covered with black molton fabric to suppress stray light. After the stated burn-in time is passed, the spectrum is measured. Calibration is performed both with a tungsten and a deuterium lamp. Both lamps were calibrated at PTB, the spectral irradiance is traceable to the International System of Units SI.

For each lamp, 100 spectral images were acquired at the lowest gain, i.e., highest signal-to-noise ratio, resulting in an integration time of 4 ms (tungsten lamp) and 700 ms (deuterium lamp) per image. It was ensured that no part of the spectrum was overexposed. The same number of dark frames were also recorded, i.e. a repetition of exactly the same measurements, except that this time the lamp was turned off. Each image was reduced separately: (1) removal of cosmic rays by a 7×1 pixel median filter (median of 7 adjacent pixels at the same wavelength), (2) extraction of the central image region of 171×2048 pixels (Czerny-Turner spectrographs are sharpest near the optical axis), (3) averaging of all 171 pixels at the same wavelength, resulting in a spectrum with a length of 2048 pixels. Finally, the 100 spectra were averaged. Then, the dark spectrum was subtracted from the light spectrum. The resulting signals are given in Fig. 3. Shown are the measured deuterium (blue) and tungsten (red) spectra and the corresponding spectral irradiances of the lamps (dashed lines). The tungsten calibration was repeated to check the stability of the calibration: the differences are less than 0.1 % and can be neglected. The relative response of the system for a given wavelength is equal to the ratio between the measured signal and the spectral irradiance of the lamp. The tungsten signal below 350 nm is too weak for reliable calibration. On the other hand, the deuterium spectrum above 370 nm has emission lines that make intensity calibration difficult. Therefore, the determination of the spectral response was split in two: up

to 360 nm it is based on the deuterium spectrum, whereas at longer wavelengths it is based on the tungsten spectrum. The resulting relative response (sensitivity) of the spectrometer/camera system is shown in Fig. 3, right. Note that there is no need to smooth the data due to the high signal-to-noise ratio.

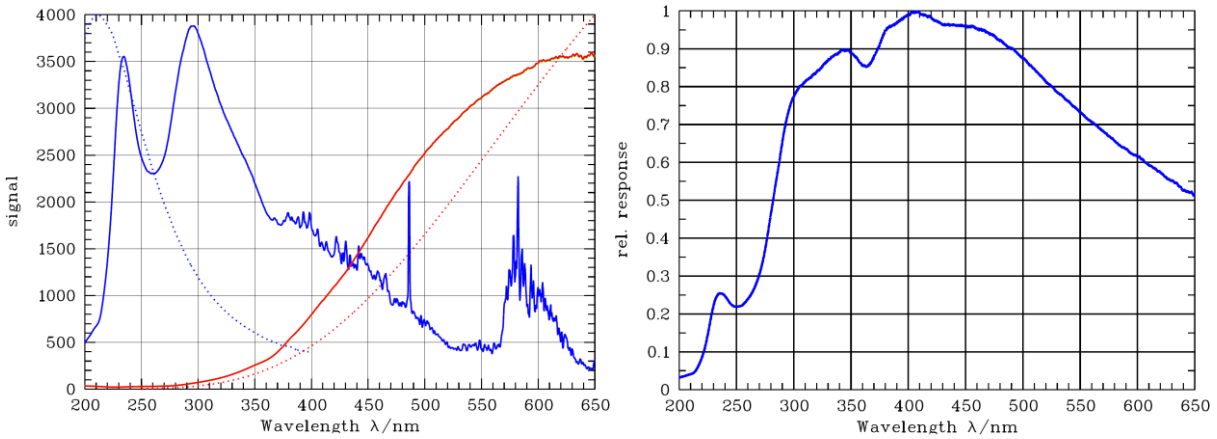

Figure 3: *Intensity calibration.* ***Left:*** *Measured spectra (solid lines) and corresponding spectral irradiance (dotted lines) of the Deuterium lamp PTB-SLD-102 (blue) and tungsten lamp PTB-KSL-006 (red).* ***Right:*** *Resulting sensitivity curve of the spectrometer/camera system.*

Below 300 nm, the sensitivity drops steeply due to the loss of efficiency of the 300 nm blazing grating. The relative minimum at 260 nm and maximum at 235 nm are due to a sensitivity minimum and maximum of the GSENSE 400BSI sensor at these wavelengths. The small drop at 360 nm is also caused by the camera. The increase from 300 nm to 400 nm is due to the increasing sensitivity of the sensor, which more than compensates for the loss of grating efficiency above 300 nm. The sensor sensitivity continues to increase up to 550 nm, but can no longer compensate for the efficiency loss of the grating. In summary, good sensitivity is achieved in the range of 270 nm to 650 nm, exactly the range required for LIF measurements at 266 nm.

The LIF spectra were acquired and reduced in exactly the same way as the intensity calibration spectra, including dark subtraction. The integration time and detector gain had to be adjusted to the LIF intensity to avoid overexposure: For acetone and 3-pentanone, 100 images á 5 s integration time were acquired with maximum gain (19.8 dB), while for toluene a shorter integration time of 1s and a gain of 17dB had to be chosen to avoid overexposure. For anisole, 500 images á 330 ms integration time were acquired with a gain of 2 dB.

The LIF intensity is calibrated by dividing by the relative response. For each intensity calibrated LIF spectrum, the total intensity is derived, which is needed for the determination of quenching effects. In addition, each spectrum was normalized to the maximum intensity above 270 nm (the 266 nm laser line is not part of the LIF spectrum and must be excluded) to simplify the comparison of the spectral shapes.

4 Results

The peak-normalized irradiance spectra are shown in Fig. 4. The measured laser intensity was 64 mJ per shot, i.e. a fluence of 1.3 mJ/mm², with a 1 σ shot-to-shot stability of better than 3 %. For all LIF spectra it was also checked whether the LIF intensity or the LIF spectrum changed over the frames of measurement, which could indicate some kind of instability or chemical reaction: neither intensity nor shape changes of the LIF spectrum were detected over time. This paper reports on an ongoing project, so measurements in H_2 and air are partially not shown. The emission lines at 266 nm and 532 nm are caused by scattered laser light and must be ignored. The LIF spectra of the tracers are discussed separately:

Acetone (Fig. 4, upper left): The smooth and broadband shape of the 266 nm LIF spectrum does not depend on the carrier gas. No quenching effect is detectable: The total intensities of the acetone in air, N_2 or H_2 LIF spectra differ by an insignificant 1 % which is within the stability limits of the laser. Hence, acetone is well-suited for concentration measurements, even in the presence of oxygen.

3-Pentanone (Fig. 4, upper right): The LIF spectrum is also independent on the carrier gas (including air), both in shape and total intensity (insignificant 1 % differences). The spectrum is not as broad as the acetone LIF spectrum and has only 40 % of the total intensity of the acetone spectrum, due to the lower vapor (saturation) pressure of 3-pentanone compared to acetone (20 hPa vs. 300 hPa at 20°C). The lower LIF signal intensity is the cause for the more prominent 532 nm laser line.

Anisole (Fig. 4, lower left): The shape of the peak-normalized anisole LIF spectrum shows no significant differences for N_2 and H_2 as carrier gas, while air causes a red shift in the peak-normalized spectrum. Moreover, a drop in the total LIF intensity above 270 nm by a factor of 17 is observed due to oxygen quenching. The stray light from the 266 nm laser line was not corrected out, hence the peak at this wavelength. The 266 nm line appears to be stronger when measured in air, but this is due to normalization to the (weaker) LIF spectrum in air.

Toluene (Fig. 4, lower right): The peak-normalized toluene LIF spectra are consistent with the literature (e.g. [6,7]). Similar to anisole, oxygen quenching causes a drop in the total LIF intensity above 270 nm of a factor of 14 (not visible in the peak-normalized spectra). It should be noted that the energy density of the laser triggers significant self-quenching of toluene [8].

Further measurements of aromatic hydrocarbons and ketones are ongoing.

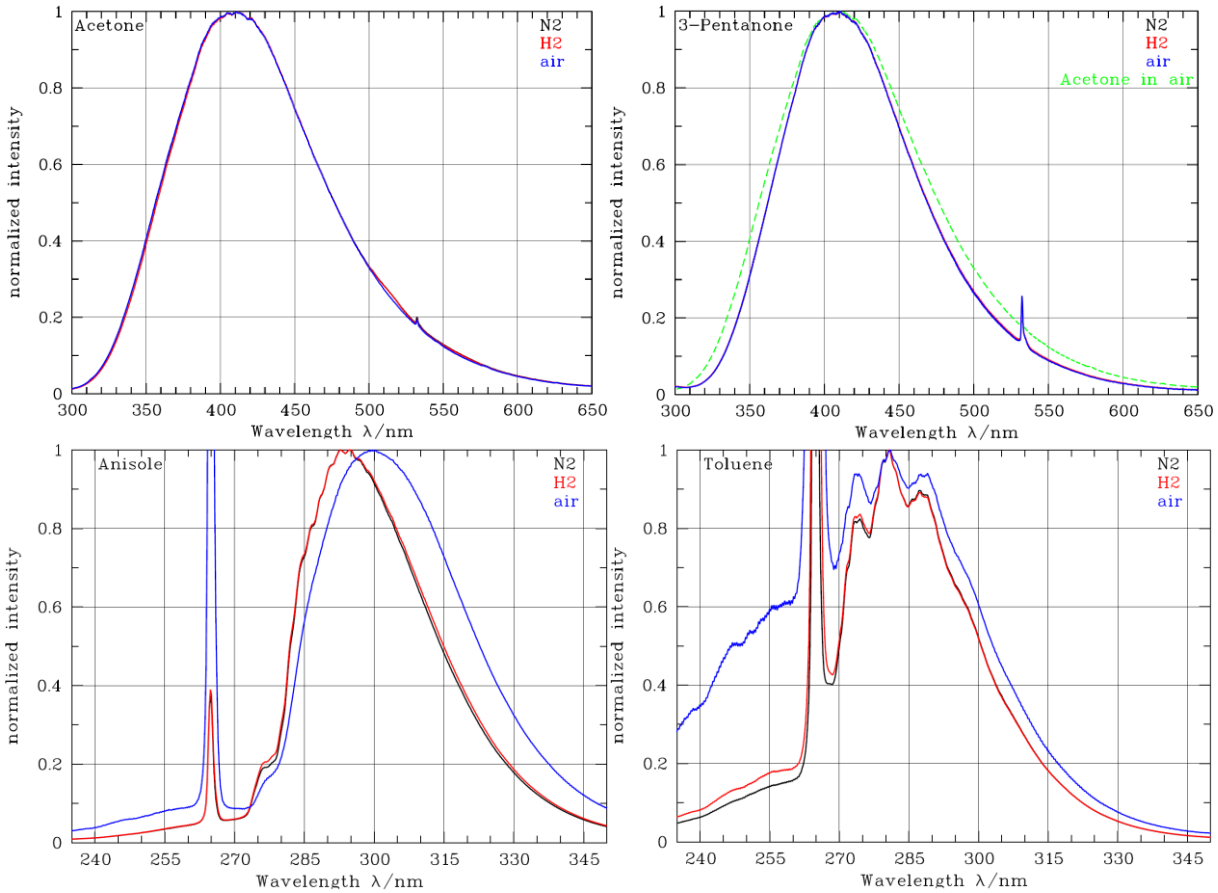

Figure 4: *266 nm normalized LIF spectra of acetone, 3-pentanone, anisole and toluene diluted in N_2 (black), H_2 (red) and dry air (blue) at 20°C (293 K) and 1 bar. The normalized acetone in air LIF spectrum is also given in the 3-pentanone plot (green) for comparison reasons.*

5 Conclusions

The present work demonstrates the advantages and capabilities of a spectrometer setup based on a modern sCMOS sensor instead of an intensified camera: higher resolution, sensitivity and linearity, lower noise level, and no sensitivity degradation at the position of the 266 nm laser line. Sample spectra of the common LIF tracer gases acetone, 3-pentanone, toluene as well as anisole are presented at ambient conditions for H_2, N_2 and air as carrier gas. Acetone and 3-pentanone are virtually insensitive to oxygen quenching (insignificant 1 % change in intensity between N_2 and air as carrier gas) and are therefore recommended for concentration measurements in the presence of oxygen. 3-pentanone provides a higher LIF signal strength per molecule than acetone, but due to its much lower vapor pressure the total intensity is lower than acetone LIF if bubblers are used. The acetone LIF spectrum is slightly broader than the 3-pentanone spectrum. Anisole and toluene have a strong oxygen quenching effect, which lowers the LIF intensity by more than an order of magnitude when air is used as carrier gas. Special attention was paid to a metrologically correct calibration of the setup. Much more information in terms of quenching, Stern-Volmer coefficients, etc. can be derived from calibrated LIF spectra than from a bandpass filter-detector combination. This paper reports on an ongoing project. Further measurements are planned, including different tracers, laser energies and excitation wavelengths, oxygen concentrations, higher temperatures and spectral resolution.

References

[1] TracerSim-Dat (2022): Open Database for Tracer-LIF Datasets, http://www.tracer-sim.com/

[2] Schulz, C.; Sick, V. (2005): "Tracer-LIF diagnostics: quantitative measurement of fuel concentration, temperature and fuel/air ratio in practical combustion systems", Prog Energy Combust Sci 31: 75

[3] Grisch, F; Thurber, M.C.; Hanson, R.K. (1997): "Mesure de température par fluorescence induite par laser sur la molécule d'acétone", Revue Scientifique et Technique de la Defense 4: 51

[4] Bryant, R.A.; Donbar, J.M.; Driscoll, J.F. (2000): "Acetone laser induced fluorescence for low pressure/low temperature flow visualization", Exp. in Fluids 28(5): 471

[5] Rossow, B. (2011): "Processus photophysiques de molécules organiques fluorescentes et du kérosène applications aux foyers de combustion : applications aux foyers de combustion", Thèse de doctorat dirigée par Gauyacq, Dolorès Chimie physique Paris 11. https://www.theses.fr/2011PA112176

[6] Yu, X.; Chang, G; Peng, J; et al. (2019): "Oxygen Concentration Distribution Measurement of the Nozzle Flow Field by Toluene/Acetone Planar Laser-Induced Fluorescence", Frontiers in Physics 7: 205

[7] Brunzendorf, J.; Diethelm, R.; Horstmann, J.; et al. (2021): „Laserinduzierte Fluoreszenzspektren von Tracergasen in Abhängigkeit von der Gaszusammensetzung", 30. Deutscher Flammentag

[8] Fuhrmann, D.; Benzler, T.; Fernando, S.; Endres, T.; Dreier, T.; Kaiser, S.A.; Schulz, C. (2017): „Self-quenching in toluene LIF", Proc. Combust. Inst. 36(3): 4505